

RESEARCH

Open Access



# The role of $^{18}\text{F}$ -FDG PET/MRI in assessing pathological complete response to neoadjuvant chemotherapy in patients with breast cancer: a systematic review and meta-analysis

Milad Ghanikolahloo<sup>1</sup>, Hayder Jasim Taher<sup>2</sup>, Ayoob Dinar Abdullah<sup>3\*</sup>, Mahsa Asadi Anar<sup>4</sup>, Ali Tayebi<sup>5</sup>, Rahil Rahimi<sup>6</sup>, Faranak Olamaeian<sup>5</sup>, Nima Rahimikashkooli<sup>7</sup> and Nima Kargar<sup>7</sup>

## Abstract

**Background and aim** The present study aimed to evaluate the use of  $^{18}\text{F}$ -2- $^{18}\text{F}$ -fluoro-2-deoxy-d-glucose (FDG) PET/MRI (Positron emission tomography-computed tomography) in predicting the pathological response to neoadjuvant chemotherapy (NAC) in patients with breast cancer (BC) compared to the use of MRI (Magnetic Resonance Imaging) alone.

**Methods** We searched numerous databases, including PubMed, Scopus, Embase, and Science Direct, using curated keywords. The variance of each study was determined using the binomial distribution, and STATA version 14 was used to analyze the data by performing random-effect models. Additionally, we calculated study heterogeneity using the chi-squared test and  $I^2$  index and utilized funnel plots and Egger tests to assess publication bias.

**Results** The current investigation analyzed 239 patients from six published studies. The pooled estimated sensitivity and specificity of  $^{18}\text{F}$ -FDG PET/MRI was 0.91 (95% CI = 0.90 to 0.92,  $I^2 = 100\%$  and  $P = 0.000$ ) and 0.62 (95% CI = 0.53 to 0.72,  $I^2 = 99.8\%$  and  $P = 0.000$ ), respectively. Pooled sensitivity and specificity of MRI were 0.78 (95% CI = 0.59 to 0.96,  $I^2 = 100\%$  and  $P = 0.000$ ) and 0.56 (95% CI = 0.33 to 0.80,  $I^2 = 99.8\%$  and  $P = 0.000$ ), respectively.

**Conclusions** Based on our findings, the combined form of  $^{18}\text{F}$ -FDG PET/MRI imaging is more sensitive and specific than MRI alone for predicting response to NAC in BC patients.

**Keywords** Neoadjuvant chemotherapy,  $^{18}\text{F}$ -FDG PET/MRI, Pathological complete response, Breast cancer

\*Correspondence:

Ayoob Dinar Abdullah  
ayoobdinara81@gmail.com

<sup>1</sup>King's College Hospital, London, England

<sup>2</sup>Department of Radiology, Hilla University College, Babylon, Iraq

<sup>3</sup>Radiology Technology Department, Al-Manara College for Medical Sciences, Missan, Iraq

<sup>4</sup>Student Research Committee, School of Medicine, Shahid Beheshti University of Medical Sciences, Tehran, Iran

<sup>5</sup>Firoozabadi Clinical Research Development Unit (FACRDU), School of Medicine, Iran University of Medical Sciences (IUMS), Tehran, Iran

<sup>6</sup>Department of Radiology, Advanced Diagnostic and Interventional Radiology Research Center, Imam Khomeini Hospital Complex, Tehran University of Medical Sciences (IUMS), Tehran, Iran

<sup>7</sup>Internal Medicine Department, School of Medicine, Shiraz University of Medical Sciences, Shiraz, Iran



© The Author(s) 2024. **Open Access** This article is licensed under a Creative Commons Attribution-NonCommercial-NoDerivatives 4.0 International License, which permits any non-commercial use, sharing, distribution and reproduction in any medium or format, as long as you give appropriate credit to the original author(s) and the source, provide a link to the Creative Commons licence, and indicate if you modified the licensed material. You do not have permission under this licence to share adapted material derived from this article or parts of it. The images or other third party material in this article are included in the article's Creative Commons licence, unless indicated otherwise in a credit line to the material. If material is not included in the article's Creative Commons licence and your intended use is not permitted by statutory regulation or exceeds the permitted use, you will need to obtain permission directly from the copyright holder. To view a copy of this licence, visit <http://creativecommons.org/licenses/by-nc-nd/4.0/>.

## Introduction

Breast cancer (BC) is the second most common disease among women worldwide and one of the most frequently diagnosed life-threatening cancers. Every year, new cases of BC are diagnosed in more than 2.3 million women, resulting in nearly 700,000 deaths [1–2].

In recent years, neoadjuvant chemotherapy (NAC) has become a standard management option for locally advanced or inflammatory BC patients. NAC can facilitate the successful implementation of breast-conserving surgery (BCS) instead of mastectomy by reducing the primary tumour size and down-staging the tumour burden before surgery [3–5]. Notably, pathologic complete response (pCR) is an important prognostic parameter for predicting disease-free survival and overall survival in patients with BC, and achieving a pCR is the best therapeutic outcome for patients receiving NAC. Hence, accurate assessment of the pCR and prediction of tumour response to NAC before surgery is crucial to avoid unnecessary surgeries in managing BC patients [1, 5].

Various effective diagnostic methods have been used in BC patients for the assessment of pathologic response to NAC, including physical examination, mammography/ultrasonography (MMG/US), positron emission tomography/computed tomography (PET/CT), magnetic resonance imaging (MRI), and pathological evaluation of the breast [6, 7]. In the meantime, noninvasive imaging techniques that can help monitor the response to NAC in BC patients are desirable. Among the radiological modalities, various international guidelines recommend breast MRI as the most accurate imaging method for monitoring treatment response and predicting patient outcomes in a neoadjuvant setting [8, 9]. However, underestimation or overestimation of residual tumor extent may be observed on breast MRI after NAC. In addition, MRI techniques cannot assess newly developing distant metastases during NAC [8]. Positron emission tomography (PET) imaging using  $^{18}\text{F}$ -2-[ $^{18}\text{F}$ ]-fluoro-2-deoxy-d-glucose ( $^{18}\text{F}$ -FDG) has an essential role in oncology as a powerful diagnostic prognostic modality, and its role in managing breast cancer is evolving.  $^{18}\text{F}$ -FDG PET method has been used to evaluate the clinical and pathological response to NAC in patients with BC, and it also shows lymph node metastasis.

Although most studies on radiomics analysis primarily utilize routine imaging techniques like CT or MRI, there is a growing trend towards employing more sophisticated imaging methods, such as multiparametric  $^{18}\text{F}$ -FDG PET/MRI. This approach aims to enhance the feature extraction process and provide a more comprehensive imaging platform. Initial results from these studies have shown promise [8]. Hence, a combined approach in the form of an  $^{18}\text{F}$ -FDG PET/MRI imaging may improve the monitoring of response to NAC and breast cancer

staging. In addition, using this hybrid, both breast and nodal status can be more accurately determined before NAC [1, 8]. Thus, the present study investigated the overall diagnostic performance and accuracy of  $^{18}\text{F}$ -FDG PET/MRI in pCR after NAC in BC patients compared to conventional MRI techniques.

## Materials and methods

We conducted this study using the PRIMSA protocol for reporting systematic reviews and meta-analyses [9].

### Search strategy

We searched the online database of PubMed, Scopus, Embase, and Science Direct from January 2000 up until December 2023 using a combination of specifically curated strategies for each database via the following keywords and Boolean operators: “positron emission tomography or positron emission tomography/ magnetic resonance imaging OR PET OR PET/MRI OR  $^{18}\text{F}$ -FDG PET/MRI,” “breast neoplasm or breast carcinoma or breast cancer or breast tumor,” “response or prediction,” and “magnetic resonance imaging or MR or MRI.” We also checked the reference list of related articles and searched Google Scholar as grey literature to prevent missing any eligible studies.

### Inclusion and exclusion criteria

The criteria for inclusion were as follows: (1) Patients should undergo both  $^{18}\text{F}$ -FDG PET/MRI scan and MRI examination before and after NAC. (2) The studies should be either prospective or retrospective. (3) The article should include a minimum of 10 patients. (4) The studies should provide raw data, including true positives (TP), false positives (FP), true negatives (TN), and false negatives (FN). (6) The gold standard for pCR should be defined as the complete absence of residual invasive tumor cells, regardless of the presence of carcinoma in situ or the absence of residual tumors and metastatic lymph nodes. (7) In MRI assessment, complete response (CR) can be defined as the absence of substantial enhancement on post-chemotherapy MR imaging or a reduction of at least 30% in the maximal diameter (D max) or volume of the tumor; (8) Parameters for PET/MRI assessment could include SUV, SUVmax, or pSUV. CR was defined as the absence of any uptake of  $^{18}\text{F}$ -FDG in the tumor, or a reduction of at least 50% in the standardized uptake value (SUV) or maximum SUV (SUV-max) or partial SUV (pSUV) compared to before NAC.

We excluded (1) review articles, editorial articles, and book chapters, and (2) articles with no FDG imaging agent, animal articles, articles that do not report sensitivity and specificity, or studies that did not simultaneously examine PET and MRI. The flow diagram (Fig. 1) shows the studies selected in this study.

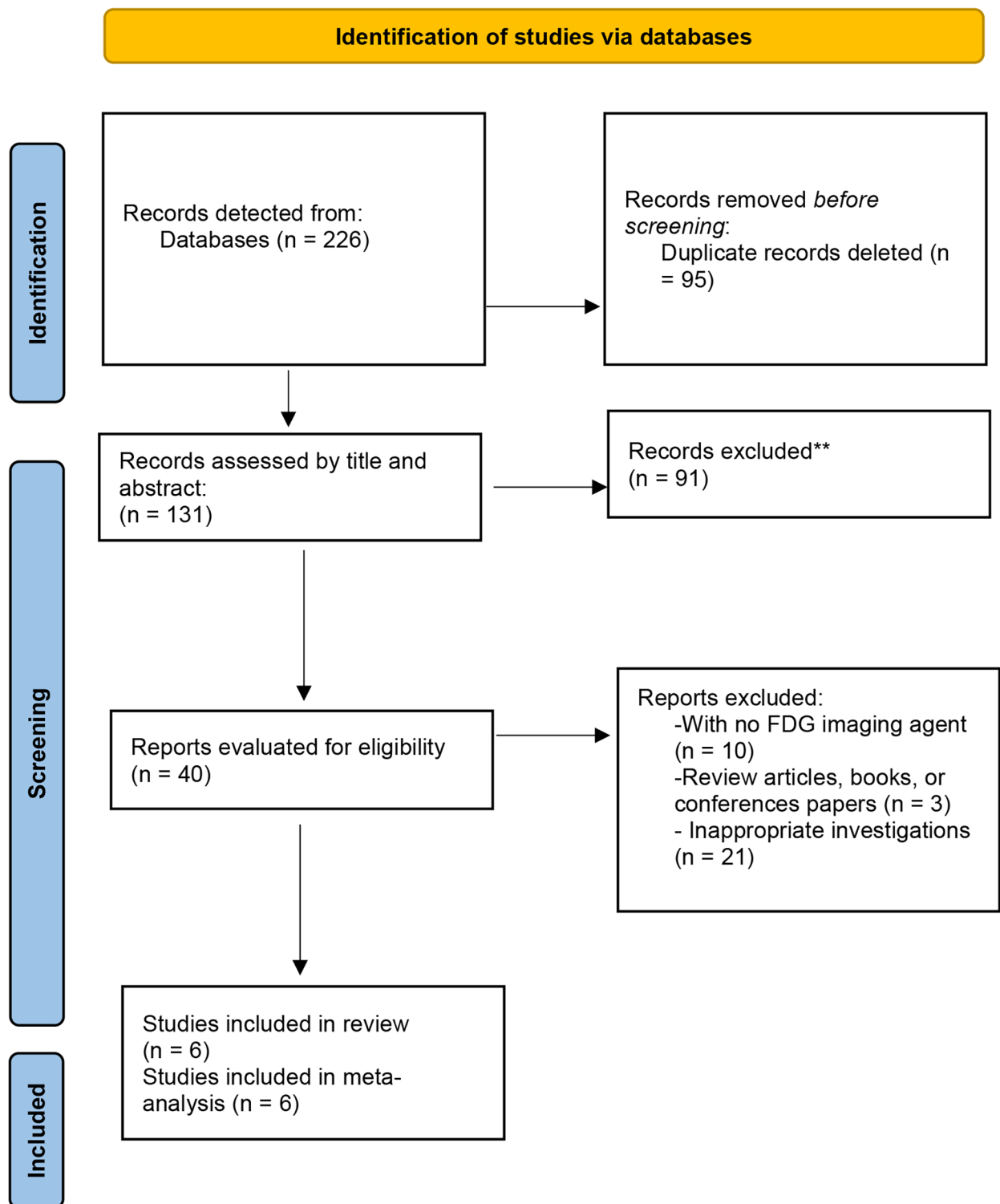


**Fig. 1** PRISMA flow diagram

### Risk of bias in individual studies (Quality assessment)

To evaluate the risk of bias in individual studies, the Newcastle–Ottawa scale (NOS) for cross-sectional and case-control studies was utilized, with 9 points for case-control studies and cohort studies indicating high quality and low risk of bias: 1–3, 4–6, and 7–9, were categorized as of low, intermediate, and high quality, respectively for case-control studies and 1–3, 4–5, and 6–9 was categorized as of low, intermediate, and high quality, respectively for cross-sectional studies (Table 1).

### Data extraction

The following data extracted from the included studies: name of the first author, place, year, sample size, mean age, design of the study, type of MRI, initial clinical stage, cancer subtype, histology subtype, evaluation index, lesion size, type of neoadjuvant chemotherapy, and specificity, sensitivity, positive predictive value (PPV), negative predictive value (NPV), and accuracy of MRI, PET, <sup>18</sup>F-FDG PET/CT, and <sup>18</sup>F-FDG PET/MRI.

### Statistical analysis

Statistical analysis was done through Stata version 14.0. The pooled sensitivity and specificity estimates were calculated using a random effects model. The standard error (S.E.) of sensitivity and specificity was calculated. The heterogeneity among different studies was analyzed using the Chi-squared test. The assessment was conducted using a forest plot, which included the presentation of  $I^2$  values. If there was heterogeneity, defined as an  $I^2$  value of more than 50%, the random effects model (REM) was chosen. Conversely, the fixed effects model (FEM) was chosen.

## Results

### Study selection

The current study is conducted according to the PRISMA checklist [10]. After the initial strategic search, 226 studies were identified. After removing duplicates and title-abstract screening, 40 studies remained for full-text screening. Finally, six studies were eligible for our meta-analysis.

### Study characteristics

The included studies were published from 2017 to 2023 [11–16]. Two studies were from the Netherlands [14, 16], one from Korea [13], one from Taiwan [15], one from Germany [12], and one from Japan [11]. The studies included 239 individuals (median sample size=42, range=10–74). The mean age of the population was 48.69 years (SD=3.97). The pathological response was considered the gold standard in the included studies. Table 2 shows the characteristics of the included studies in detail.

### Performance of PER/MRI, MRI, and PET in evaluating response to neoadjuvant chemotherapy

The estimated pooled sensitivity and specificity of <sup>18</sup>F-FDG PET/MRI was 0.91 (95% CI=0.90 to 0.92,  $I^2=100%$  and  $P=0.000$ ), and 0.62 (95% CI=0.53 to 0.72,  $I^2=99.8%$  and  $P=0.000$ ), respectively (Fig. 2). Pooled sensitivity and specificity of MRI were 0.78 (95%CI=0.59 to 0.96,  $I^2=100%$  and  $P=0.000$ ) and 0.56 (95%CI=0.33 to 0.80,  $I^2=99.8%$  and  $P=0.000$ ), respectively (Fig. 3).

The pooled estimate of PPV and NPV of <sup>18</sup>F-FDG PET/MRI were 0.92 (95%CI=0.91 to 0.93,  $I^2=100%$  and  $P=0.000$ ) and 0.63 (95%CI=0.47 to 0.79,  $I^2=99.9%$  and  $P=0.000$ ), respectively. The PPV and NPV of MRI were 0.75 (95%CI=0.54 to 0.96,  $I^2=100%$  and  $P=0.000$ ) and 0.66 (95% CI=0.61 to 0.71,  $I^2=98.6%$   $P=0.000$ ).

**Table 1** Quality assessment of included studies

Author (Reference)	Selection				Comparability of cohorts based on the design or analysis	Outcome			Over- all score
	Representa- tiveness of the exposed cohort	Selection of the non- exposed cohort	Ascertain- ment of exposure	Demonstration that outcome of interest was not present at the start of the study		Assess- ment of outcome	Was follow- up long enough for out- comes to occur	Adequacy of follow- up of cohorts	
Sekine [11]	*	*	*	*	**	*	*	*	9
Cho [13]	*	*	*		**	*	*	*	8
de Mooij [14]	*	*	*			*	*		5
Wang [15]	*	*	*		**	*	*	*	8
de Mooij [16]	*	*	*		**	*		*	7
Umutlu [12]			*	*	**	*		*	6

**Table 2** Characteristics of the included studies

First Author	Country	Year	Sample size	Mean age (Range/ Years)	Study design	Types of MRI Sequences	Name of scanner	Initial clinical stage	Subtype of Cancer	Histology subtype	Evaluation index	Lesion size (mm)	Type of NAC
Sekine (11)	Japan	2021	74	48 (30-78)	Retrospective	T1-weighted sequence (T1W), T2-weighted sequence (T2W), along with dynamic contrast-enhanced imaging,	a-Se full-field digital mammography (FFDM) system with a spatial resolution of 85 µm (MAM-MOMAT Inspiration, Siemens)	T1 (13), T2 (48), T3 (11), T4 (2)	HR+/HER2 (30), HR+/HER2+ (16), HR/HER2+ (10), HR/HER2 (18)	IDC (71), ILC (1), Metaplastic carcinoma (2)	FFDG PET/MRI	0.36	Most patients (72 out of 74) were treated with an anthracycline-based regimen followed by a taxane regimen. For patients with HER2-positive disease, the NAC regimen was augmented with targeted therapies: All patients with HER2-positive disease received trastuzumab as part of their treatment. One patient with HER2-positive disease also received pertuzumab in addition to trastuzumab. Two patients received a platinum-based regimen followed by a taxane regimen, which included:
Umutlu (12)	Germany	2022	73	49 (Range 27-77 years)	Retrospective	T2-weighted fat-saturated TSE, diffusion-weighted EPI, and dynamic contrast-enhanced T1-weighted FLASH.	Biograph mMR, Siemens Healthcare GmbH, Erlangen, Germany	G1 (1), G2 (37), G3 (35)	Basal-like/triple-negative (19), Luminal A (10), Luminal B (42), Her2-enriched (2)	NST (69), Lobular invasive (3), Other (1)	18 F-FDG PET/MRI PET		NR
Cho (13)	Republic of Korea	2017	26	42.2	Prospective	axial Dixon-VIBE and coronal HASTE.	Biograph mMR; Siemens Healthcare, Erlangen, Germany	II (5), III (21)	Hormone receptor-positive (15), Triple-negative (4), HER2-positive (7)		18 F-FDG PET/MRI PET	0.49	For HER2-Negative Disease: NAC Regimen: Combination of anthracyclines and taxanes. For HER2-Positive Disease: NAC Regimen: Chemotherapy incorporating HER2-targeted agents (e.g., trastuzumab and/or pertuzumab).

**Table 2** (continued)

First Author	Country	Year	Sample size	Mean age (Range/ Years)	Study design	Types of MRI Sequences	Name of scanner	Initial clinical stage	Subtype of Cancer	Histology subtype	Evaluation index	Lesion size (mm)	Type of NAC
de Mooij (14)	Netherlands	2022	10	50.3	Prospective	unenanced T1-weighted (T1W), unenhanced T2-weighted (T2W), and the PET sequence.	Siemens Healthcare, Erlangen, Germany	I (1), II (5), III (4)	ER (6), PR (4), HER2 (5)	NST (9), Mixed NST, and ILC (1)	18 F-FDG PET/ MRI T1-weighted imaging T2-weighted imaging PET		For HER2-Negative Patients: Option 1: Taxanes (docetaxel or paclitaxel) followed by epirubicin and cyclophosphamide, with or without fluorouracil. Option 2: Fluorouracil, epirubicin, and cyclophosphamide (or epirubicin and cyclophosphamide) followed by taxanes. For HER2-Positive Patients: Option 1: Taxanes in combination with trastuzumab, followed by fluorouracil, epirubicin, and cyclophosphamide (or epirubicin and cyclophosphamide). Option 2: Concurrent regimen of taxanes, cyclophosphamide, trastuzumab, and pertuzumab. Option 3: Carboplatin in combination with taxanes, trastuzumab, and pertuzumab.
Wang (15)	Taiwan	2017	14	54.5	NR	10 sequences (3 precontrast, 6 DCE-MRI postcontrast, 1 MRS) PET Sequences: 1 main sequence for breast PET imaging with attenuation correction	-	T1 (1), T2 (11), T3 (2)	Lum A (2), Lum B (1), HER2 positive (8), TNBC (3)		PET/MR(SUVmax/ ADCmin) PET/MR (TLG/ADCmin)	0.36	For HER2-Negative Patients: Option 1: Taxanes (docetaxel or paclitaxel) followed by epirubicin and cyclophosphamide, with or without fluorouracil. Option 2: Fluorouracil, epirubicin, and cyclophosphamide (or epirubicin and cyclophosphamide) followed by taxanes. For HER2-Positive Patients: Option 1: Taxanes in combination with trastuzumab, followed by fluorouracil, epirubicin, and cyclophosphamide (or epirubicin and cyclophosphamide). Option 2: Concurrent regimen of taxanes, cyclophosphamide, trastuzumab, and pertuzumab. Option 3: Carboplatin in combination with taxanes, trastuzumab, and pertuzumab.

**Table 2** (continued)

First Author	Country	Year	Sample size	Mean age (Range/ Years)	Study design	Types of MRI Sequences	Name of scanner	Initial clinical stage	Subtype of Cancer	Histology subtype	Evaluation index	Lesion size (mm)	Type of NAC
de Mooij (16)	Netherlands	2023	42	50	Prospective	Axial DWI (EPI and CHES) Pre-contrast dynamic contrast-enhanced axial T1WI (VIBRANT and CHES) Post-contrast dynamic contrast-enhanced axial T1WI (90 s phase) Post-contrast dynamic contrast-enhanced axial T1WI (180 s phase) Post-contrast dynamic contrast-enhanced axial T1WI (270 s phase)	Biograph mMR; Siemens Healthineers, Erlangen, Germany	I (4), II (22), III (16)	ER+/HER2- (19), ER+/HER2+ (7), ER-/HER2+ (6), TNBC (10)		18 F-FDG PET/ MRI MRI PET	0.34	For ER-Positive and/or HER2-Positive Breast Cancer: Initial Regimen: 4 cycles of doxorubicin and cyclophosphamide, administered every 3 weeks. Subsequent Regimen: 4 cycles of docetaxel, administered every 3 weeks. Targeted Therapy: For HER2-positive cases, trastuzumab was included in the regimen. Additionally, one or more patients received pertuzumab along with trastuzumab. For Triple-Negative (TN) Breast Cancer: Regimen: 12 cycles of weekly doses of paclitaxel.

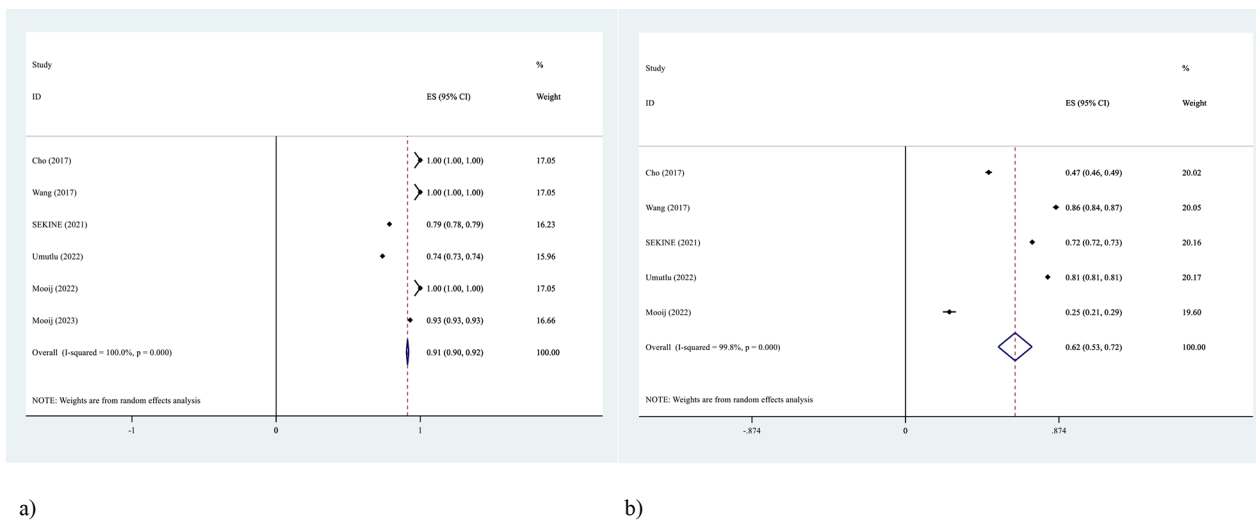


**Fig. 2** Forest plots showing the pooled estimate of specificity (a) and sensitivity (b) of <sup>18</sup>F-FDG PET/MRI in Assessing pCR to NAC in patients with breast cancer. The square represents the effect estimate of individual studies with more than 95% confidence intervals (CI)). The size of the squares is proportional to the weight assigned to the study in the meta-analysis. Diamond denotes the overall estimation

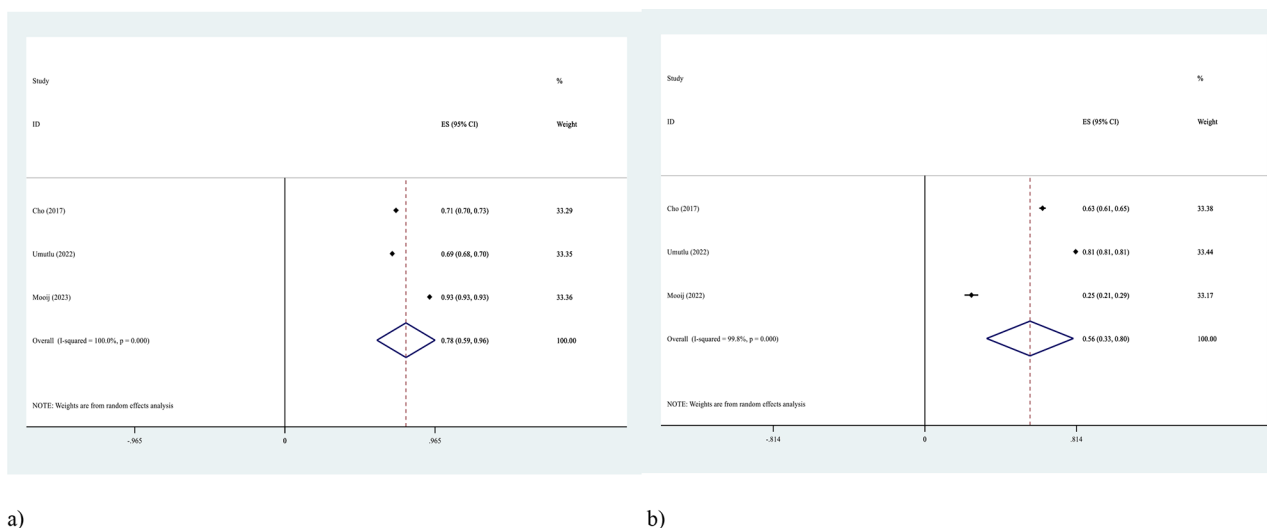


**Fig. 3** Forest plots showing the pooled estimate of sensitivity (a) and specificity (b) of MRI in Assessing pCR to NAC in patients with breast cancer, The square represents the effect estimate of individual studies with more than 95% confidence intervals (95% CI), with the size of squares proportional to the weight assigned to the study in the meta-analysis. Diamond denotes the overall estimation

**Publication bias**

Begg’s test, which we performed, revealed no indication of publication bias among the included articles ( $p=0.322$ ). The publication bias funnel plot for the included papers is shown in Fig. 4.

**Discussion**

Traditional anatomical imaging methods, such as mammograms and breast ultrasound, have traditionally been performed to evaluate the pathologic response of BC to NAC. However, these anatomical imaging modalities can sometimes be challenging in determining response to NAC. It is difficult to differentiate between fibrosis and

residual tumors with these methods, and their use is limited in monitoring the treatment response [5, 17]. <sup>18</sup>F-FDG PET and MRI imaging are increasingly employed to predict and monitor BC patients’ pathological response to NAC. A hybrid form of <sup>18</sup>F-FDG PET/MRI imaging modalities could be attractive due to the possibility of improving the monitoring of the response to NAC treatment, staging of cancer, and the accuracy of nodal status assessment in BC [8, 18].

This study systematically assessed the diagnostic performance and accuracy of MRI and combined <sup>18</sup>F-FDG PET/MRI in pCR after NAC in BC patients. In the study of Tokuda et al. [19], the sensitivity and specificity of two

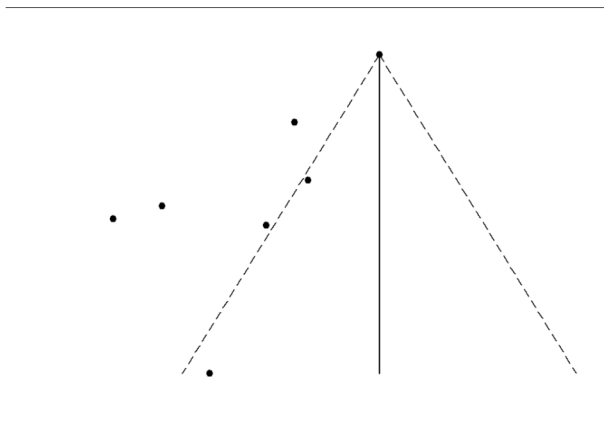


**Fig. 4** Funnel plot among the studies

imaging modalities of dedicated breast PET (dbPET) and whole-body PET (WBPET) in predicting pCR after NAC was reported as 85.7% and 72.7%, 71.4% and 77.3%, respectively. The reduction rate (R.R.) of peak standardized uptake values (SUVp) may significantly influence the results. In the study by KIM et al. [20], when an R.R. of 88% was used as the threshold value for distinguishing between pCR and pPR (pathological partial response), the sensitivity and specificity of FDG-PET for predicting the pathological response of BC to NAC were 100% and 56.5%, respectively. While with R.R. of 79%, sensitivity and specificity were reported as 85.2% and 82.6%, respectively.

MRI results in our study revealed a specificity and sensitivity of 78% and 56%, respectively, for predicting the response to NAC therapy in patients with BC. In another meta-analysis study, results revealed a higher sensitivity (65% vs. 56%) and specificity (88% vs. 78%) of MRI in assessing pCR to NAC in patients with BC compared with ours [18]. In the study by Wu et al. [21] to evaluate and predict the pathological response to NAC in BC patients, the sensitivity and specificity for diffusion-weighted MRI (DWI) were 93% and 82%, and for dynamic contrast-enhanced MRI (DCE-MRI) were reported as 56% and 78%, respectively. A previous study showed the sensitivity and specificity of the DCE-MRI imaging method to be 100% and 50%, respectively [19]. The difference in the results can be due to the difference in the type of MRI modality and depending on the SUV cut-off value as a significant influencing factor.

Our study introduced the hybrid form  $^{18}\text{F}$ -FDG PET/MRI imaging with 62% sensitivity and 91% specificity as a more powerful prognostic tool for predicting response to NAC treatment in B.C. patients than MRI alone because, during NAC, the metabolic reduction in the tumor occurs much earlier than the vascularization and shrinking of the tumor volume. Metabolic analysis may only

investigate the initial effect of NAC, and by integrating it with morphology and vascular analysis, a more accurate prediction may be possible [11, 22, 23]. Hence, the hybrid form of  $^{18}\text{F}$ -FDG PET/MRI can help improve the accuracy of NAC therapy assessment in BC because clinicians can simultaneously collect morphological and metabolic imaging information.

Although our study introduced  $^{18}\text{F}$ -FDG PET/MRI imaging as a useful prognostic tool in predicting response to NAC in BC, it has some limitations. (1) In the studies we included in our meta-analysis, there can be heterogeneity in the different types and stages of breast cancer. (2) MRI technique may vary among the studies reviewed and affect the results. (3) Despite each imaging method's diagnostic value, the investigated strategies' monetary value still needs to be examined as it is a costly procedure in many countries and comes with an unavailable approach. (4) The breast cancer subtypes included are heterogeneous. However, the subgroups' responses to chemotherapy and pet-CT sensitivity are unequal. For instance, the lobular histological type produces weaker PET-CT uptake. Additionally, triple negatives have a good NAC response. Applying subgroup analysis will increase the quality of findings in future research (0.5) we observed high heterogeneity amongst included articles that need to be further addressed in future studies when the data on the current literature reaches a higher level of considerability.

## Conclusion

The results of our study showed that the combined form of  $^{18}\text{F}$ -FDG PET/MRI imaging has higher sensitivity and specificity for predicting response to NAC in BC patients than MRI alone. Therefore, this study highlights the importance of using the  $^{18}\text{F}$ -FDG PET/MRI modality as a powerful prognostic tool in BC that can improve the accuracy of pCR assessment after NAC.

## Acknowledgements

None.

## Author contributions

Conceptualization: MGH, RAB, and ADB; Methodology, Supervision, and Writing original draft, review, and editing: MGH, HJT, AT, MAA, RR, and FO; Formal analysis and investigation: NRR, NK, AND SHY.

## Funding

No fund received.

## Data availability

No datasets were generated or analysed during the current study.

## Declarations

### Ethics approval and consent to participate

not applicable.

### Consent for publication

Not applicable.

### Competing interests

The authors declare no competing interests.

Received: 3 April 2024 / Accepted: 13 August 2024

Published online: 19 November 2024

### References

1. Wilkinson L, Gathani T. Understanding breast cancer as a global health concern. *Br J Radiol*. 2022;95(1130):20211033.
2. Arnold M, Morgan E, Rumgay H et al. Current and future burden of breast cancer: Global statistics for 2020 and 2040. *The Breast*, vol. 66, pp. 15–23, 2022.
3. Sarhan EAS, El Gohary MI, El Moneim LA, Ali SA. Role of 18 fluorine-fluorodeoxyglucose positron emission tomography/computed tomography in the assessment of neoadjuvant chemotherapy response in breast cancer patients. *Egypt J Radiol Nuclear Med*. 2020;51(1):1–10.
4. Yang L, Chang J, He X et al. PET/CT-based radiomics analysis may help to predict neoadjuvant chemotherapy outcomes in breast cancer. *Quant Imaging Artif Intell Breast Tumor Diagnosis*, 16648714, pp.282, 2023.
5. Li H, Yao L, Jin P, et al. MRI and PET/CT for evaluation of the pathological response to neoadjuvant chemotherapy in breast cancer: a systematic review and meta-analysis. *Breast*. 2018;40:106–15.
6. Han S, Choi JY. Prognostic value of 18 F-FDG PET and PET/CT for assessment of treatment response to neoadjuvant chemotherapy in breast cancer: a systematic review and meta-analysis. *Breast Cancer Res*. 2020;22:1–15.
7. Dobruch-Sobczak K, Piotrkowska-Wróblewska H, Klimonda Z, et al. Multiparametric ultrasound examination for response assessment in breast cancer patients undergoing neoadjuvant therapy. *Sci Rep*. 2021;11(1):2501.
8. Goorts B, Vöö S, van Nijnatten TJ et al. Hybrid 18 F-FDG PET/MRI might improve locoregional staging of breast cancer patients prior to neoadjuvant chemotherapy. *Eur J Nucl Med Mol Imaging*, 44, pp. 1796–805, 2017.
9. Dobruch-Sobczak K, Piotrkowska-Wróblewska H, Klimoda Z, et al. Monitoring the response to neoadjuvant chemotherapy in patients with breast cancer using ultrasound scattering coefficient: a preliminary report. *J Ultrasonography*. 2019;19(77):89–97.
10. Liberati A, Altman DG, Tetzlaff J, et al. The PRISMA statement for reporting systematic reviews and meta-analyses of studies that evaluate health care interventions: explanation and elaboration. *J Clin Epidemiol*. 2009;62(10):e1–34.
11. Sekine C, Uchiyama N, Watase C, et al. Preliminary experiences of PET/MRI in predicting complete response in patients with breast cancer treated with neoadjuvant chemotherapy. *Mol Clin Oncol*. 2022;16(2):50.
12. Umutlu L, Kirchner J, Bruckmann NM et al. Multiparametric (18)F-FDG PET/MRI-Based Radiomics for Prediction of Pathological Complete Response to Neoadjuvant Chemotherapy in Breast Cancer. *Cancers (Basel)*, vol. 14, no. 7, 2022.
13. Cho N, Im SA, Cheon GJ et al. Integrated (18)F-FDG PET/MRI in breast cancer: early prediction of response to neoadjuvant chemotherapy. *Eur J Nucl Med Mol Imaging*, vol. 45, no. 3, pp. 328–39, 2018.
14. de Mooij CM, Samiei S, Mitea C et al. Axillary lymph node response to neoadjuvant systemic therapy with dedicated axillary hybrid (18)F-FDG PET/MRI in clinically node-positive breast cancer patients: a pilot study. *Clin Radiol*, 77, 10, pp. e732–e40, 2022.
15. Wang J, Shih TT, Yen RF. Multiparametric Evaluation of Treatment Response to neoadjuvant chemotherapy in breast Cancer using Integrated PET/MR. *Clin Nucl Med*, 42, 7, pp. 506–13, 2017.
16. de Mooij CM, van Nijnatten TJA, Goorts B et al. Prediction of primary Tumor and Axillary Lymph Node response to Neoadjuvant Chemo(targeted) therapy with dedicated breast [18F]FDG PET/MRI in breast Cancer. *Cancers (Basel)*, 15, 2, 2023.
17. Kitajima K, Miyoshi Y. Present and future role of FDG-PET/CT imaging in the management of breast cancer. *Japanese J Radiol*. 2016;34:167–80.
18. Liu Q, Wang C, Li P, Liu J, Huang G, Song S. The role of 18F-FDG PET/CT and MRI in assessing pathological complete response to neoadjuvant chemotherapy in patients with breast cancer: a systematic review and meta-analysis. *Biomed Res Int*, 2016.
19. Tokuda Y, Yanagawa M, Fujita Y, et al. Prediction of pathological complete response after neoadjuvant chemotherapy in breast cancer: comparison of diagnostic performances of dedicated breast PET, whole-body PET, and dynamic contrast-enhanced MRI. *Breast Cancer Res Treat*. 2021;188:107–15.
20. Kim SJ, Kim Sk, Lee E, Ro J, Kang S. Predictive value of [18F] FDG PET for pathological response of breast cancer to neo-adjuvant chemotherapy. *Ann Oncol*. 2004;15(9):1352–7.
21. Wu LM, Hu JN, Gu HY, et al. Can diffusion-weighted MR imaging and contrast-enhanced MR imaging precisely evaluate and predict pathological response to neoadjuvant chemotherapy in patients with breast cancer? *Breast Cancer Res Treat*. 2012;135:17–28.
22. Kim TH, Yoon JK, Kang DK et al. Value of volume-based metabolic parameters for predicting survival in breast cancer patients treated with neoadjuvant chemotherapy. *Medicine*, 95, 41, 2016.
23. Rice SL, Friedman KP. Clinical PET-MR imaging in breast cancer and lung cancer. *PET Clin*. 2016;11(4):387–402.

### Publisher's Note

Springer Nature remains neutral with regard to jurisdictional claims in published maps and institutional affiliations.